# Test of Lepton Flavor Universality with $B_s^0 \to \phi \ell^+ \ell^-$ Decays

R. Aaij *et al.*[*]
(LHCb Collaboration)

(Received 18 October 2024; revised 12 February 2025; accepted 13 February 2025; published 27 March 2025)

Lepton flavor universality in rare $b \to s$ transitions is tested for the first time using $B_s^0$ meson decays. The measurements are performed using $pp$ collision data collected by the LHCb experiment between 2011 and 2018, corresponding to a total integrated luminosity of 9 $\mathrm{fb}^{-1}$. Branching fraction ratios between the $B_s^0 \to \phi e^+ e^-$ and $B_s^0 \to \phi \mu^+ \mu^-$ decays are measured in three regions of dilepton mass squared, $q^2$, with $0.1 < q^2 < 1.1$, $1.1 < q^2 < 6.0$, and $15 < q^2 < 19\ \mathrm{GeV}^2/c^4$. The results agree with the standard model expectation of lepton flavor universality.

DOI: 10.1103/PhysRevLett.134.121803

The decay of a $B_s^0$ meson to a $\phi$ meson and pair of oppositely charged leptons, $\ell^+\ell^-$, involves a $b$- to $s$-quark flavor-changing neutral-current transition. Such processes are rare in the standard model of particle physics (SM). In extensions of the SM, the rates of these processes could be modified by the contribution of as-yet undiscovered particles. The branching fraction of the $B_s^0 \to \phi \mu^+ \mu^-$ decay, $\mathcal{B}(B_s^0 \to \phi \mu^+ \mu^-)$, has been measured by the CDF [1] and LHCb [2–4] Collaborations as a function of the dilepton mass squared, $q^2$. The experimental measurements are systematically below theoretical predictions, with a local tension as large as 3.6 standard deviations [4]. However, comparisons with theoretical predictions are complicated by sizeable uncertainties on the form factors for the $B_s^0 \to \phi$ transition [5,6] and hadronic corrections to the decay rate [7,8]. Discrepancies with SM predictions have also been found in the angular distributions of the $B_s^0 \to \phi \mu^+ \mu^-$ decay [9], as well as in the rate and angular distribution of other $b \to s \mu^+ \mu^-$ transitions [10–18]. This pattern of tensions with SM predictions has led to significant discussion within the community [19–34].

Lepton flavor universality tests, which compare the rates of processes involving different flavors of charged leptons, can provide powerful probes of the SM. In such comparisons, SM uncertainties associated with hadronic form factors largely cancel and, since the electroweak couplings are flavor universal, processes are expected to differ only by phase-space and QED effects [35,36]. In some extensions of the SM, this accidental flavor-symmetry could be violated (see, for example, Refs. [37–40]).

In this Letter, a first measurement of the lepton universality ratio $R_\phi = \mathcal{B}(B_s^0 \to \phi \mu^+ \mu^-)/\mathcal{B}(B_s^0 \to \phi e^+ e^-)$ is reported. Inclusion of charge-conjugate processes is implied throughout. The analysis uses data from $pp$ collisions at center-of-mass energies of $\sqrt{s} = 7$, 8, and 13 TeV, corresponding to a total integrated luminosity of 9 $\mathrm{fb}^{-1}$, collected by the LHCb Collaboration between 2011 and 2018. Measurements are performed in three bins of $q^2$: $0.1 < q^2 < 1.1$ (low), $1.1 < q^2 < 6.0$ (central), and $15 < q^2 < 19\ \mathrm{GeV}^2/c^4$ (high). The lowest $q^2$ bin contains small contributions from light-quark resonances decaying to $\ell^+\ell^-$ (predominantly the $\rho(770)^0$ and $\phi$ mesons). Similar tests involving $B^{\{+,0\}} \to K^{\{+,0\}} \ell^+ \ell^-$, $B^{\{+,0\}} \to K^{*\{+,0\}} \ell^+ \ell^-$ and $\Lambda_b^0 \to p K^- \ell^+ \ell^-$ decays have previously been performed by the *BABAR* [41], Belle [42], CMS [17], and LHCb Collaborations [43–49]. One advantage of performing tests with $B_s^0 \to \phi \ell^+ \ell^-$ decays is that the clean signature of the $\phi \to K^+ K^-$ decay significantly reduces most sources of background. This facilitates the inclusion of the high-$q^2$ bin, which has not been studied in previous LHCb publications.

The analysis strategy follows closely the approach described in Refs. [48,49]. To reduce systematic uncertainties on the modeling of the lepton reconstruction efficiency, the double ratio of branching fractions,

$$R_\phi = \left( \frac{\mathcal{B}(B_s^0 \to \phi \mu^+ \mu^-)}{\mathcal{B}(B_s^0 \to J/\psi(\to \mu^+ \mu^-)\phi)} \right) \Bigg/ \left( \frac{\mathcal{B}(B_s^0 \to \phi e^+ e^-)}{\mathcal{B}(B_s^0 \to J/\psi(\to e^+ e^-)\phi)} \right), \tag{1}$$

---

[*] Full author list given at the end of the Letter.

is measured. Here, each individual branching fraction is obtained as the corresponding yield in the relevant $q^2$ interval divided by its efficiency, with other multiplicative factors that cancel exactly in Eq. (1). In practice, $R_\phi^{-1}$ is measured rather than $R_\phi$ such that the small $B_s^0 \to \phi e^+e^-$ yield appears in the numerator and the statistical behavior of the observable more closely follows a Gaussian distribution. To avoid experimenter's bias, the $B_s^0 \to \phi e^+e^-$ candidates with masses in the range 5.2–5.5 $\mathrm{GeV}/c^2$ (slightly different for each $q^2$ interval), the corresponding signal yields, and $R_\phi^{-1}$ are not inspected until all aspects of the analysis procedure are finalized.

The LHCb detector [50,51] is a single-arm forward spectrometer covering the pseudorapidity range $2 < \eta < 5$, designed for the study of particles containing $b$ or $c$ quarks. The detector includes a high-precision tracking system, comprising silicon-strip [52,53] and straw drift-tube [54] detectors. Different types of charged hadrons are distinguished using information from two ring-imaging Cherenkov detectors [55]. Electrons are identified using a calorimeter system comprising scintillating-pad and preshower detectors, an electromagnetic, and a hadronic calorimeter. Muons are identified by a system composed of alternating layers of iron and multiwire proportional chambers [56]. The online event selection is performed by a trigger [57], which consists of a hardware and a software stage.

Simulated data samples are used to determine the efficiency of the event reconstruction and candidate selection, which is needed to determine the branching fractions from the observed yields. These samples are also used to understand candidate mass line shapes, and the contributions from different background sources. In the simulation, $pp$ collisions are generated using PYTHIA [58] with a specific LHCb configuration [59]. Decays of unstable particles are described by EVTGEN [60], in which final-state radiation is generated using PHOTOS [61]. Simulated $B_s^0 \to \phi\ell^+\ell^-$ decays are generated according to a model based on Refs. [62–64]. The interactions of the generated particles with the detector, and its response, are simulated using the GEANT4 toolkit [65] as described in Ref. [66]. The simulated samples are corrected to account for known data-simulation differences in the $B_s^0$ production kinematics and detector occupancy, as well as track reconstruction, particle identification, and trigger efficiencies. The $q^2$ distribution of the simulated $B_s^0 \to \phi e^+e^-$ sample is smeared to better match the resolution of the $B_s^0 \to J/\psi\phi$ candidates in data.

The analysis uses data triggered at the hardware stage either by particles in the event that are not used to form signal candidates, or by an electron (muon) with large transverse energy (transverse momentum) for $B_s^0 \to \phi e^+e^-$ ($B_s^0 \to \phi\mu^+\mu^-$) decays. The $E_\mathrm{T}$ ($p_\mathrm{T}$) thresholds vary in the ranges 2.4–3.0 GeV (1.5–2.9 $\mathrm{GeV}/c$). In the subsequent software trigger, events are retained if they contain at least one reconstructed track that has a large $p_\mathrm{T}$ and is significantly displaced from every primary proton-proton interaction vertex (PV). This track is then combined with at least one other track to form a vertex and events are retained based on topological criteria [67,68]. Off-line, $B_s^0 \to \phi\ell^+\ell^-$ candidates are formed by combining two leptons of opposite charge with a pair of kaons of opposite charge. A dedicated algorithm is used to correct for the bremsstrahlung emission of the electrons, associating energy deposits in the calorimeter to electrons based on their trajectories. Candidates are accepted if their reconstructed mass is in the range $5000 < m(K^+K^-\mu^+\mu^-) < 6000$ or $4600 < m(K^+K^-e^+e^-) < 6600\ \mathrm{MeV}/c^2$ and if the kaon pair has a mass within $\pm 12\ \mathrm{MeV}/c^2$ of the known $\phi$ meson mass [69]. Contributions in this mass region from $B_s^0 \to K^+K^-\ell^+\ell^-$ decays, where the kaons do not originate from a $\phi$ meson, are known to be small and are neglected [4]. The leptons and kaons must have significant impact parameter (IP) values and form a common vertex that is displaced from every PV. The PV that fits best to the $B_s^0$ flight direction is taken as the associated PV, and the $B_s^0$ candidate must have a small IP with respect to this PV. In the $B_s^0 \to \phi\mu^+\mu^-$ sample, candidates with dimuon masses within $\pm 100\ \mathrm{MeV}/c^2$ of the known $J/\psi$ mass are assumed to originate from $B_s^0 \to J/\psi\phi$ decays. A wider range, $6 < q^2 < 11\ \mathrm{GeV}^2/c^4$, is used for $B_s^0 \to J/\psi(\to e^+e^-)\phi$ decays to account for the worse mass resolution resulting from bremsstrahlung and the associated energy recovery procedure.

Combinatorial backgrounds are suppressed using a gradient boosted decision tree (BDT) classifier [70]. The classifier uses topological and kinematic information, including: the chi square of a common vertex fit to the four particles, the consistency of the $B_s^0$ candidate with originating from the associated PV, the displacement of the candidate's decay vertex from that PV, its $p_\mathrm{T}$, and the $p_\mathrm{T}$ and IP of the kaons and the leptons. Separate classifiers are trained for the dielectron and dimuon final states and for the 2011–2012, 2015-–2016, and 2017–2018 run periods. Simulated signal decays and candidates from upper mass sidebands, with $m(K^+K^-\mu^+\mu^-) > 5400$ and $m(K^+K^-e^+e^-) > 5600\ \mathrm{MeV}/c^2$, are used as signal and background proxies in the training. To increase the amount of data available for training and avoid biases, $k$-fold cross validation [71] with $k = 10$ is used for the training or testing samples. The working points of the classifier are chosen to optimize the precision on an $R_\phi$ measurement based on the measured $B_s^0 \to \phi\mu^+\mu^-$ branching fraction [4], assuming $R_\phi = 1$. Working points are optimized separately for the three $q^2$ regions.

The narrow window around the $\phi$ meson mass reduces the background from many specific $b$-hadron decays. Backgrounds from $B^0 \to K^{*0}(\to K^+\pi^-)\ell^+\ell^-$ and $\Lambda_b^0 \to pK^-\ell^+\ell^-$ decays are reduced to a negligible level by particle identification requirements. Potential background from $B_s^0 \to D_s^-(\to \phi\pi^-)\ell^+\nu_\ell$ decays, where the $\pi^-$ is mistakenly identified as a lepton, is rejected by removing candidates if the $\phi\ell^-$ mass is consistent with that of a $D_s^-$ meson after the pion mass has been assigned to the lepton. This veto also removes potential background from $B_s^0 \to D_s^-(\to \phi\pi^-)\pi^+$ decays with double misidentification. Additional particle identification criteria are applied to remove $b$-hadron decays to $J/\psi$ or $\psi(2S)$ mesons and two charged hadrons, where a hadron is mistakenly reconstructed as a lepton and vice versa. These criteria are applied for $B_s^0 \to \phi\mu^+\mu^-$ candidates if the mass formed by the hadron and muon of opposite charge is consistent with the $J/\psi$ or $\psi(2S)$ mass when the hadron is assigned the muon mass. For $B_s^0 \to \phi e^+e^-$ candidates the criteria are applied if the four-body mass, calculated with the electron mass assigned to the $K^\pm$, and the $e^\pm$ assigned either the pion, kaon or proton mass, is close to that of a known $b$ hadron.

The $\phi\ell^+\ell^-$ final state has relatively few potential backgrounds from partially reconstructed $b$-hadron decays with missing hadrons. The most relevant are $B^{\{0,+\}} \to \phi K^{\{0,+\}}\ell^+\ell^-$ decays where the kaon is not reconstructed. Backgrounds from hadronic $b$ decays, where two charged hadrons are misidentified as leptons and potentially one or more hadrons are not reconstructed, are poorly known. The contribution from these backgrounds is estimated using the same data-driven approach as employed in Refs. [48,49].

A separate BDT classifier is trained to reject background in the high-$q^2$ interval from $J/\psi \to e^+e^-$ decays originating from a $b$ hadron, where bremsstrahlung photons have been incorrectly assigned to the electrons, or incorrectly reconstructed. The BDT classifier is trained using simulated events and uses information on the bremsstrahlung photon energy, reconstructed track momentum, track asymmetries, and the dielectron mass. The classifier achieves a signal efficiency of 90% while rejecting more than 80% of these backgrounds.

After applying the full selection less than 0.3% of events contain more than one candidate, in which case a single candidate is selected at random. The yields of $B_s^0 \to \phi\ell^+\ell^-$ and $B_s^0 \to J/\psi\phi$ decays are determined by performing unbinned extended maximum-likelihood fits to the mass distributions of the candidates in the different samples, using ZFIT [72]. The fit is performed simultaneously, where $R_\phi^{-1}$ is shared over the different data-taking periods. The $B_s^0 \to \phi\ell^+\ell^-$ and $B_s^0 \to J/\psi\phi$ signals are described by modified Gaussian functions with power-law tails. The functions have different width and tail parameters on the left- and right-hand sides of the distribution. For $B_s^0 \to \phi e^+e^-$ decays, the line shape is obtained by summing functions that represent the cases where either zero, one, or two or more calorimeter clusters are associated with bremsstrahlung from the dielectron pair. The fractional contribution of these functions is validated to agree well between data and simulation using the $B_s^0 \to J/\psi\phi$ sample. These fractions are then fixed from simulation, together with the tail parameters of the signal shapes, in the fit to data. The peak and width parameters for each $q^2$ bin are taken from simulation but are allowed to vary by scale factors in the fits to the data. For the $B_s^0 \to \phi\ell^+\ell^-$ samples, the scale factors are constrained to match those of the corresponding $B_s^0 \to J/\psi\phi$ samples.

Combinatorial background in the low- and central-$q^2$ bins is described by an exponential function using independent slope parameters in the different $q^2$ regions. The combinatorial shape is modified at high $q^2$, by multiplying the exponential function by a sigmoid function to account for the reduced $q^2$ range available at low $m(K^+K^-\ell^+\ell^-)$. The shape of the sigmoid is determined from a model where $m(K^+K^-\ell^+\ell^-)$ and $q^2$ are described by exponential functions, which are parameterized using candidates at large $m(K^+K^-\ell^+\ell^-)$. It is verified with data that there is negligible correlation between the $q^2$ and $m(K^+K^-\ell^+\ell^-)$ distributions.

Background from semileptonic decays of a $B_s^0$ to a $D_s^-$ meson, where the $D_s^-$ also decays semileptonically, is modeled by an exponential function with a slope parameter fixed from simulation. This background is only present in the low- and central-$q^2$ bins. The shape and level of background from misidentified hadrons are obtained by combining three control regions in data, where either one or both leptons are selected with particle identification criteria favoring hadrons, following the procedure in Refs. [48,49].

For the fit to the dielectron samples, additional background components, with parameters fixed from simulation, are included to account for leakage from $B_s^0 \to J/\psi\phi$ [$B_s^0 \to \psi(2S)\phi$] decays into the central- and high-$q^2$ (high-$q^2$ only) bins. In central $q^2$, the $B_s^0 \to J/\psi\phi$ leakage is described by a Gaussian function. At high $q^2$, the $B_s^0 \to J/\psi\phi$ and $B_s^0 \to \psi(2S)\phi$ leakage shapes are described by a nonparametric kernel density estimate and by a Johnson $S_U$ function [73], respectively. For the $B_s^0 \to J/\psi\phi$ samples, background components below the 1% level are included to describe $B^0 \to J/\psi K^{*0}$, $\Lambda_b^0 \to J/\psi pK^-$, and $B^0 \to J/\psi\phi$ decays. These components are taken nonparametrically from simulated samples. The yields of semileptonic, leakage, and misidentified backgrounds are each constrained in the fits to estimates from simulation.

Figure 1 shows the mass distributions of selected $B_s^0 \to \phi e^+e^-$ candidates in the different $q^2$ bins. The corresponding mass distributions for selected $B_s^0 \to \phi\mu^+\mu^-$ candidates, which are similar to those in Ref. [4], are provided as Appendixes. The yields of the $B_s^0 \to \phi e^+e^-$ ($B_s^0 \to \phi\mu^+\mu^-$) decays in the low-, central-, and high-$q^2$ bin are $63 \pm 9$ ($159 \pm 13$), $119 \pm 14$ ($300 \pm 18$), and $50 \pm 13$ ($312 \pm 18$), respectively. The lower yield for the dielectron compared to the dimuon modes is due to lower track-reconstruction

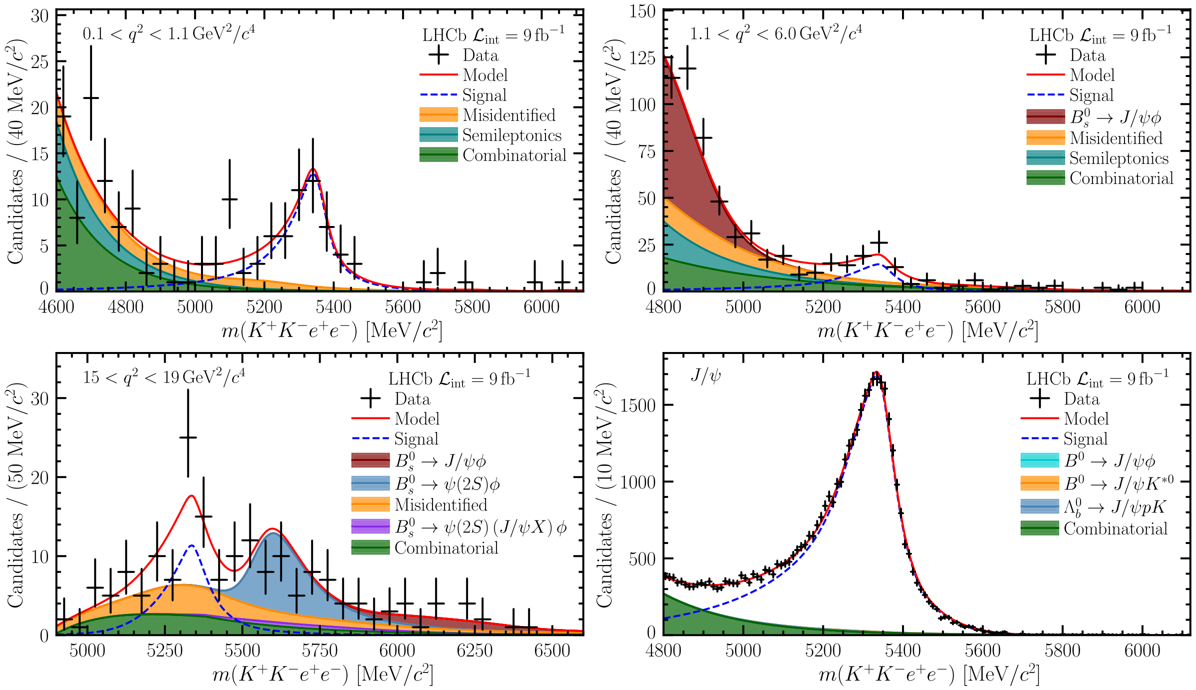

FIG. 1. Mass distributions of selected $B_s^0 \to \phi e^+e^-$ candidates in the (top left) low-, (top right) central-, (bottom left) high-$q^2$, and (bottom right) $J/\psi$ bins. The data are summed over the three data-taking periods and are compared with the result of the fit described in the text.

efficiency for electrons and the large $E_{\mathrm{T}}$ requirement necessary to select them in the hardware trigger. The statistical significance of the $B_s^0 \to \phi e^+e^-$ signal in the three $q^2$ bins is determined using Wilks's theorem [74] to correspond to 6.8, 5.4, and 3.6 standard deviations ($\sigma$).

The analysis is validated using pseudoexperiments, generated with $R_\phi = 1$ and taking $\mathcal{B}(B_s^0 \to \phi\mu^+\mu^-)$ from Ref. [4]. The resulting fits are found to have good coverage and bias at the level of 10% of the statistical uncertainty or less. The bias is corrected and the uncertainty on the bias assigned as a source of systematic uncertainty. Several cross-checks are performed to validate the analysis using data. The branching fraction of the $B_s^0 \to \phi\mu^+\mu^-$ decay is measured and found to be consistent with Ref. [4]. Consistent values of $R_\phi^{-1}$ are found when analyzing the data with stricter particle identification requirements. The $B_s^0 \to J/\psi\phi$ yields are also determined from fits to the candidate mass distribution with the $\ell^+\ell^-$ mass constrained to the known mass of the $J/\psi$ meson. This significantly improves the mass resolution on the $B_s^0 \to J/\psi\phi$ samples but only changes the yields by 0.2%, confirming that the $K^+K^-\ell^+\ell^-$ mass model gives an appropriate description of the data. The ratio of branching fractions between $B_s^0 \to J/\psi(\to \mu^+\mu^-)\phi$ and $B_s^0 \to J/\psi(\to e^+e^-)\phi$ decays, $r_{J/\psi}$, is determined from fits to the constrained masses, in bins of different kinematic variables, and found to be consistent with unity; the most significant variation is used to assign a systematic uncertainty on the measurement of $R_\phi^{-1}$. The value of $r_{J/\psi}$ for the combined dataset is $r_{J/\psi} = 0.997 \pm 0.013$, where the uncertainty combines the statistical and a subset of the systematic uncertainties pertaining to the limited size of the calibration samples used in the data-simulation corrections. The double ratio $R_{\psi(2S)}$, defined by replacing the signal mode $B_s^0 \to \phi\ell^+\ell^-$ with the decay $B_s^0 \to \psi(2S)\phi$ in Eq. (1), is determined from fits to candidates with $11 < q^2 < 15\ \mathrm{GeV}^2/c^4$. The double ratio is found to

TABLE I. Sources of systematic uncertainty in $10^{-2}$ on the $R_\phi^{-1}$ measurement in the low-, central-, and high-$q^2$ bins. The total uncertainty is computed by combining the contributions from individual sources in quadrature.

| Source $[10^{-2}]$ | Low | Central | High |
|---|---|---|---|
| Fit bias | < 0.1 | 0.9 | 1.4 |
| Normalization | 0.2 | 0.2 | 0.2 |
| $r_{J/\psi}$ variation | 1.3 | 0.6 | 0.9 |
| Efficiency calibration | 0.7 | 0.5 | 1.2 |
| $q^2$ smearing | 0.6 | 0.5 | 0.3 |
| Decay model | 0.1 | 0.3 | 0.1 |
| Signal line shape | 1.7 | 1.5 | 3.7 |
| Misidentified background | 4.1 | 4.3 | 7.4 |
| Combinatorial background | ⋯ | ⋯ | 3.9 |
| Leakage background | ⋯ | 0.9 | 2.1 |
| Semileptonic background | 1.3 | 1.2 | ⋯ |
| Total | 4.9 | 4.9 | 9.6 |

TABLE II. Values of $R_\phi^{-1}$ and $\mathrm{d}\mathcal{B}(B_s^0 \to \phi e^+ e^-)/\mathrm{d}q^2$ in the low-, central-, and high-$q^2$ bins. The first uncertainty is statistical and the second systematic. For the differential branching fraction, the third and the fourth uncertainty are due to the experimental uncertainty on the ratio $\mathrm{d}\mathcal{B}(B_s^0 \to \phi\mu^+\mu^-)/\mathrm{d}q^2/\mathcal{B}(B_s^0 \to J/\psi\phi)$ [4] and on $\mathcal{B}(B_s^0 \to J/\psi\phi)$ [69,78], respectively.

| $q^2$ (GeV$^2/c^4$) | $R_\phi^{-1}$ | $\mathrm{d}\mathcal{B}(B_s^0 \to \phi e^+ e^-)/\mathrm{d}q^2$ ($10^{-7}$ GeV$^{-2}$ $c^4$) |
|---|---|---|
| $0.1 < q^2 < 1.1$ | $1.57^{+0.28}_{-0.25} \pm 0.05$ | $1.38^{+0.25}_{-0.22} \pm 0.04 \pm 0.19 \pm 0.06$ |
| $1.1 < q^2 < 6.0$ | $0.91^{+0.20}_{-0.19} \pm 0.05$ | $0.26 \pm 0.06 \pm 0.01 \pm 0.01 \pm 0.01$ |
| $15.0 < q^2 < 19.0$ | $0.85^{+0.24}_{-0.23} \pm 0.10$ | $0.39 \pm 0.11 \pm 0.04 \pm 0.02 \pm 0.02$ |

be $R_{\psi(2S)} = 1.010 \pm 0.026$, consistent with the expectation of unity, where again the uncertainty combines statistical and systematic contributions. An independent test [75] using $\phi$ mesons from $D_s^+$ decays, that decay to $e^+e^-$ and $\mu^+\mu^-$, shows that the lepton efficiency is well understood even for lower momentum leptons.

The different sources of systematic uncertainty on $R_\phi^{-1}$ considered in the analysis are summarized in Table I. Sources of uncertainty on the efficiencies, related to the finite size of the simulation and variations of the data-simulation corrections, impact $R_\phi^{-1}$ at the ~1% level. Small variations of the decay model used in the simulation, accounting for the time dependence of the signal decay rate, have a minimal impact on $R_\phi^{-1}$. Variations of the $q^2$ resolution also impact the efficiency calculation as simulated decays migrate into and out of the $q^2$ bins used in the analysis. A systematic uncertainty on the $q^2$ -resolution correction is determined by evaluating separate correction factors from the $B_s^0 \to J/\psi\phi$ sample in bins of electron $p_\mathrm{T}$. Modifying the correction factors changes $R_\phi^{-1}$ by less than 1%.

The largest sources of systematic uncertainty are associated with the modeling of the signal and background in the likelihood fits. The uncertainty associated with the signal line shape is estimated by replacing the model by a simplified function, with a single Gaussian core, and by varying the fractions of the different bremsstrahlung categories that form the line shape. The uncertainty on the modeling of misidentified hadronic backgrounds is determined by varying both the size and shape of the contribution in the fit. Variations are made to the particle-identification requirements used to define the background-like control regions, the efficiency maps that translate yields in the backgroundlike regions to yields in the signal region, and in the model used to parametrize the line shape. The effect of the finite size of the backgroundlike samples is assessed using a bootstrapping technique [76]. Uncertainty on the high-$q^2$ combinatorial-background shape is evaluated by varying the shape of the $q^2$ distribution used to determine the sigmoid parameters, and by replacing the model by an alternate function with a power-law turn-on and exponential falloff, with parameters constrained from a fit to data with same-sign $\ell^\pm\ell^\pm$ or $K^\pm K^\pm$ combinations. An uncertainty from the $J/\psi$ and $\psi(2S)$ leakage into the central- and high-$q^2$ bins is assigned by replacing the parametric shapes by a nonparametric model, varying the constraints on the background yields in the fit, and by varying the $q^2$ resolution in the simulation. An uncertainty associated with the semileptonic background is evaluated by estimating the effects of replacing the background model by a nonparametric model and varying the background level.

The $R_\phi^{-1}$ values in the three $q^2$ ranges are given in Table II. The results are in good agreement with the SM expectation. Figure 2 shows the variation with $R_\phi^{-1}$ of the difference in log-likelihood of the fit from the best fit point. For low $q^2$, a local minimum around $R_\phi^{-1} \sim 1.3$ yields a nonparabolic profile likelihood towards lower $R_\phi^{-1}$ values. The presence of this additional minimum is evident when considering the variation of the likelihood in the full parameter space and is induced by large correlations between the combinatorial background and the signal model in combination with the small sample size. Depending on the $m(K^+K^-e^+e^-)$ mass range, the particle identification criteria and BDT requirement, the minimum

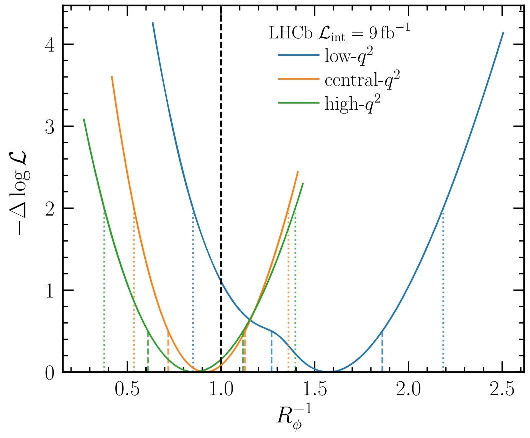

FIG. 2. Profile log-likelihood of $R_\phi^{-1}$ for the low-, central-, and high-$q^2$ bins, relative to the best fit point. Systematic uncertainties are included by convolving the likelihood from the fit with a Gaussian distribution of width equal to the systematic uncertainty. The vertical lines indicate the $1\sigma$ and $2\sigma$ confidence intervals, respectively.

at $R_{\phi}^{-1} \sim 1.3$ can be favored. The $2\sigma$ interval on $R_{\phi}^{-1}$ from the profile likelihood is [0.86, 2.18]; the results is in agreement at the level of $1.4\sigma$ with a SM prediction of 1.016 computed using Ref. [77]. Table II also presents the differential branching fraction of the $B_s^0 \to \phi e^+ e^-$ decay, determined from $R_{\phi}^{-1}$, $\mathrm{d}\mathcal{B}(B_s^0 \to \phi\mu^+\mu^-)/\mathrm{d}q^2/\mathcal{B}(B_s^0 \to J/\psi\phi)$ [4] and $\mathcal{B}(B_s^0 \to J/\psi\phi)$ [69,78]. The upper value of the low-$q^2$ range in Ref. [4] is extrapolated from 0.98 to 1.1 $\mathrm{GeV}^2/c^4$ by assuming that $\mathrm{d}\mathcal{B}(B_s^0 \to \phi\mu^+\mu^-)/\mathrm{d}q^2$ is uniform in $q^2$. At $2\sigma$, $\mathrm{d}\mathcal{B}(B_s^0 \to \phi e^+ e^-)/\mathrm{d}q^2$ in the low-$q^2$ region is in the range $[0.65, 2.08] \times 10^{-7}\ \mathrm{GeV}^{-2}\, c^4$. As implied by $R_{\phi}^{-1}$, the $B_s^0 \to \phi e^+ e^-$ branching fraction is consistent with that of the $B_s^0 \to \phi\mu^+\mu^-$ decay and lies below the central value of the SM prediction in the central- and high-$q^2$ bins.

In summary, the first measurement of the ratio of $B_s^0 \to \phi e^+ e^-$ and $B_s^0 \to \phi\mu^+\mu^-$ branching fractions is presented. This represents the first test of lepton flavor universality with $B_s^0 \to \phi\ell^+\ell^-$ decays. It is also the most precise test of lepton flavor universality in the high-$q^2$ region of any measurement involving $b \to s\ell^+\ell^-$ transitions. Together with Ref. [79], this result constitutes the first observation of the $B_s^0 \to \phi e^+ e^-$ decay. In addition, the differential branching fraction of the $B_s^0 \to \phi e^+ e^-$ decay is measured in three bins of $q^2$. The results are statistically limited and agree with the SM expectation of lepton flavor universality, placing important constraints on extensions of the SM.

*Acknowledgments*—We express our gratitude to our colleagues in the CERN accelerator departments for the excellent performance of the LHC. We thank the technical and administrative staff at the LHCb institutes. We acknowledge support from CERN and from the national agencies: CAPES, CNPq, FAPERJ, and FINEP (Brazil); MOST and NSFC (China); CNRS/IN2P3 (France); BMBF, DFG, and MPG (Germany); INFN (Italy); NWO (Netherlands); MNiSW and NCN (Poland); MCID/IFA (Romania); MICIU and AEI (Spain); SNSF and SER (Switzerland); NASU (Ukraine); STFC (United Kingdom); DOE NP and NSF (U.S.). We acknowledge the computing resources that are provided by CERN, IN2P3 (France), KIT and DESY (Germany), INFN (Italy), SURF (Netherlands), PIC (Spain), GridPP (United Kingdom), CSCS (Switzerland), IFIN-HH (Romania), CBPF (Brazil), and Polish WLCG (Poland). We are indebted to the communities behind the multiple open-source software packages on which we depend. Individual groups or members have received support from ARC and ARDC (Australia); Key Research Program of Frontier Sciences of CAS, CAS PIFI, CAS, CCEPP, Fundamental Research Funds for the Central Universities, and Sci. & Tech. Program of Guangzhou (China); Minciencias (Colombia); EPLANET, Marie Skłodowska-Curie Actions, ERC and NextGenerationEU (European Union); A*MIDEX, ANR, IPhU, and Labex P2IO, and Région Auvergne-Rhône-Alpes (France); AvH Foundation (Germany); ICSC (Italy); Severo Ochoa and María de Maeztu Units of Excellence, GVA, XuntaGal, GENCAT, InTalent-Inditex and Prog. Atracción Talento CM (Spain); SRC (Sweden); the Leverhulme Trust, the Royal Society and UKRI (United Kingdom).

[1] T. Aaltonen *et al.* (CDF Collaboration), Observation of the baryonic flavor-changing neutral current decay $\Lambda_b \to \Lambda\mu^+\mu^-$, Phys. Rev. Lett. **107**, 201802 (2011).

[2] R. Aaij *et al.* (LHCb Collaboration), Differential branching fraction and angular analysis of the decay $B_s^0 \to \phi\mu^+\mu^-$, J. High Energy Phys. 07 (2013) 084.

[3] R. Aaij *et al.* (LHCb Collaboration), Angular analysis and differential branching fraction of the decay $B_s^0 \to \phi\mu^+\mu^-$, J. High Energy Phys. 09 (2015) 179.

[4] R. Aaij *et al.* (LHCb Collaboration), Branching fraction measurements of the rare $B_s^0 \to \phi\mu^+\mu^-$ and $B_s^0 \to f_2'(1525)\mu^+\mu^-$ decays, Phys. Rev. Lett. **127**, 151801 (2021).

[5] R. R. Horgan, Z. Liu, S. Meinel, and M. Wingate, Lattice QCD calculation of form factors describing the rare decays $B \to K^*\ell^+\ell^-$ and $B_s \to \phi\ell^+\ell^-$, Phys. Rev. D **89**, 094501 (2014).

[6] A. Bharucha, D. M. Straub, and R. Zwicky, $B \to V\ell^+\ell^-$ in the standard model from light-cone sum rules, J. High Energy Phys. 08 (2016) 098.

[7] M. Ciuchini *et al.*, $B \to K^*\ell^+\ell^-$ decays at large recoil in the standard model: A theoretical reappraisal, J. High Energy Phys. 06 (2016) 116.

[8] N. Gubernari, M. Reboud, D. van Dyk, and J. Virto, Improved theory predictions and global analysis of exclusive $b \to s\mu^+\mu^-$ processes, J. High Energy Phys. 09 (2022) 133.

[9] R. Aaij *et al.* (LHCb Collaboration), Angular analysis of the rare decay $B_s^0 \to \phi\mu^+\mu^-$, J. High Energy Phys. 11 (2021) 043.

[10] R. Aaij *et al.* (LHCb Collaboration), Differential branching fractions and isospin asymmetries of $B \to K^{(*)}\mu^+\mu^-$ decays, J. High Energy Phys. 06 (2014) 133.

[11] A. M. Sirunyan *et al.* (CMS Collaboration), Measurement of angular parameters from the decay $B^0 \to K^{*0}\mu^+\mu^-$ in proton-proton collisions at $\sqrt{s} = 8$ TeV, Phys. Lett. B **781**, 517 (2018).

[12] M. Aaboud *et al.* (ATLAS Collaboration), Angular analysis of $B_d^0 \to K^*\mu^+\mu^-$ decays in $pp$ collisions at $\sqrt{s} = 8$ TeV with the ATLAS detector, J. High Energy Phys. 10 (2018) 047.

[13] R. Aaij *et al.* (LHCb Collaboration), Measurement of $CP$ -averaged observables in the $B^0 \to K^{*0}\mu^+\mu^-$ decay, Phys. Rev. Lett. **125**, 011802 (2020).

[14] R. Aaij *et al.* (LHCb Collaboration), Angular analysis of the $B^+ \to K^{*+}\mu^+\mu^-$ decay, Phys. Rev. Lett. **126**, 161802 (2021).

[15] R. Aaij *et al.* (LHCb Collaboration), Amplitude analysis of the $B^0 \to K^{*0}\mu^+\mu^-$ decay, Phys. Rev. Lett. **132**, 131801 (2024).

[16] R. Aaij *et al.* (LHCb Collaboration), Comprehensive analysis of local and nonlocal amplitudes in the $B^0 \to K^{*0}\mu^+\mu^-$ decay, J. High Energy Phys. 09 (2024) 026.

[17] A. Hayrapetyan *et al.* (CMS Collaboration), Test of lepton flavor universality in $B^\pm \to K^\pm\mu^+\mu^-$ and $B^\pm \to K^\pm e^+e^-$ decays in proton-proton collisions at $\sqrt{s} = 13$ TeV, Rep. Prog. Phys. **87**, 077802 (2024).

[18] A. Hayrapetyan *et al.* (CMS Collaboration), Angular analysis of the $B^0 \to K^{*0}(892)\mu^+\mu^-$ decay in proton-proton collisions at $\sqrt{s} = 13$ TeV, arXiv:2411.11820.

[19] A. Crivellin and B. Mellado, Anomalies in particle physics and their implications for physics beyond the standard model, Nat. Rev. Phys. **6**, 294 (2024).

[20] B. Capdevila, A. Crivellin, and J. Matias, Review of semileptonic B anomalies, Eur. Phys. J. Spec. Top. **1**, 20 (2023).

[21] P. Athron, R. Martinez, and C. Sierra, $B$ meson anomalies and large $B^+ \to K^+\nu\bar{\nu}$ in non-universal $\mathrm{U}(1)'$ models, J. High Energy Phys. 02 (2024) 121.

[22] B. Allanach and A. Mullin, Plan B: New $Z'$ models for $b \to s\ell^+\ell^-$ anomalies, J. High Energy Phys. 09 (2023) 173.

[23] J. Davighi and B. A. Stefanek, Deconstructed hypercharge: A natural model of flavour, J. High Energy Phys. 11 (2023) 100.

[24] G. Isidori, Z. Polonsky, and A. Tinari, Semi-inclusive $b \to s\bar{\ell}\ell$ transitions at high $q^2$, Phys. Rev. D **108**, 093008 (2023).

[25] M. Ciuchini *et al.*, Constraints on lepton universality violation from rare $B$ decays, Phys. Rev. D **107**, 055036 (2023).

[26] A. Greljo, J. Salko, A. Smolkovič, and P. Stangl, Rare $b$ decays meet high-mass Drell-Yan, J. High Energy Phys. 05 (2023) 087.

[27] N. R. Singh Chundawat, *CP* violation in $b \to s\ell\ell$: A model independent analysis, Phys. Rev. D **107**, 075014 (2023).

[28] W. G. Parrott, C. Bouchard, and C. T. H. Davies (HPQCD Collaboration), Standard Model predictions for $B \to K\ell^+\ell^-$, $B \to K\ell_1^-\ell_2^+$ and $B \to K\nu\bar{\nu}$ using form factors from $N_f = 2+1+1$ lattice QCD, Phys. Rev. D **107**, 014511 (2023); **107**, 119903(E) (2023).

[29] M. Fernández Navarro and S. F. King, B-anomalies in a twin Pati-Salam theory of flavour including the 2022 LHCb $R_{K^{(*)}}$ analysis, J. High Energy Phys. 02 (2023) 188.

[30] N. R. Singh Chundawat, New physics in $B \to K^*\tau^+\tau^-$: A model independent analysis, Phys. Rev. D **107**, 055004 (2023).

[31] B. Allanach and J. Davighi, The rumble in the meson: A leptoquark versus a $Z'$ to fit $b \to s\mu^+\mu^-$ anomalies including 2022 LHCb $R_{K^{(*)}}$ measurements, J. High Energy Phys. 04 (2023) 033.

[32] R. Bause, H. Gisbert, M. Golz, and G. Hiller, Model-independent analysis of $b \to d$ processes, Eur. Phys. J. C **83**, 419 (2023).

[33] M. Ciuchini *et al.*, Charming penguins and lepton universality violation in $b \to s\ell^+\ell^-$ decays, Eur. Phys. J. C **83**, 64 (2023).

[34] M. Algueró *et al.*, To (b)e or not to (b)e: No electrons at LHCb, Eur. Phys. J. C **83**, 648 (2023).

[35] M. Bordone, G. Isidori, and A. Pattori, On the standard model predictions for $R_K$ and $R_{K^*}$, Eur. Phys. J. C **76**, 440 (2016).

[36] G. Isidori, D. Lancierini, S. Nabeebaccus, and R. Zwicky, QED in $\bar{B} \to \bar{K}\ell^+\ell^-$ LFU ratios: theory versus experiment, a Monte Carlo study, J. High Energy Phys. 10 (2022) 146.

[37] G. Hiller and F. Kruger, More model-independent analysis of $b \to s$ processes, Phys. Rev. D **69**, 074020 (2004).

[38] S. L. Glashow, D. Guadagnoli, and K. Lane, Lepton flavor violation in $B$ decays?, Phys. Rev. Lett. **114**, 091801 (2015).

[39] I. Doršner *et al.*, Physics of leptoquarks in precision experiments and at particle colliders, Phys. Rep. **641**, 1 (2016).

[40] D. Buttazzo, A. Greljo, G. Isidori, and D. Marzocca, B-physics anomalies: A guide to combined explanations, J. High Energy Phys. 11 (2017) 044.

[41] J. P. Lees *et al.* (*BABAR* Collaboration), Measurement of branching fractions and rate asymmetries in the rare decays $B \to K^{(*)}l^+l^-$, Phys. Rev. D **86**, 032012 (2012).

[42] S. Choudhury *et al.* (Belle Collaboration), Test of lepton flavor universality and search for lepton flavor violation in $B \to K\ell\ell$ decays, J. High Energy Phys. 03 (2021) 105.

[43] R. Aaij *et al.* (LHCb Collaboration), Test of lepton universality using $B^+ \to K^+\ell^+\ell^-$ decays, Phys. Rev. Lett. **113**, 151601 (2014).

[44] R. Aaij *et al.* (LHCb Collaboration), Test of lepton universality with $B^0 \to K^{*0}\ell^+\ell^-$ decays, J. High Energy Phys. 08 (2017) 055.

[45] R. Aaij *et al.* (LHCb Collaboration), Test of lepton universality using $\Lambda_b^0 \to pK^-\ell^+\ell^-$ decays, J. High Energy Phys. 05 (2020) 040.

[46] R. Aaij *et al.* (LHCb Collaboration), Test of lepton universality in beauty-quark decays, Nat. Phys. **18**, 277 (2022).

[47] R. Aaij *et al.* (LHCb Collaboration), Tests of lepton universality using $B^0 \to K_S^0\ell^+\ell^-$ and $B^+ \to K^{*+}\ell^+\ell^-$ decays, Phys. Rev. Lett. **128**, 191802 (2022).

[48] R. Aaij *et al.* (LHCb Collaboration), Measurement of lepton universality parameters in $B^+ \to K^+\ell^+\ell^-$ and $B^0 \to K^{*0}\ell^+\ell^-$ decays, Phys. Rev. D **108**, 032002 (2023).

[49] R. Aaij *et al.* (LHCb Collaboration), Test of lepton universality in $b \to s\ell^+\ell^-$ decays, Phys. Rev. Lett. **131**, 051803 (2023).

[50] A. A. Alves Jr. *et al.* (LHCb Collaboration), The LHCb detector at the LHC, J. Instrum. **3**, S08005 (2008).

[51] R. Aaij *et al.* (LHCb Collaboration), LHCb detector performance, Int. J. Mod. Phys. A **30**, 1530022 (2015).

[52] R. Aaij *et al.*, Performance of the LHCb vertex locator, J. Instrum. **9**, P09007 (2014).

[53] R. Arink *et al.*, Performance of the LHCb outer tracker, J. Instrum. **9**, P01002 (2014).

[54] P. d'Argent *et al.*, Improved performance of the LHCb Outer Tracker in LHC Run 2, J. Instrum. **12**, P11016 (2017).

[55] M. Adinolfi *et al.*, Performance of the LHCb RICH detector at the LHC, Eur. Phys. J. C **73**, 2431 (2013).

[56] A. A. Alves Jr. *et al.*, Performance of the LHCb muon system, J. Instrum. **8**, P02022 (2013).

[57] R. Aaij *et al.*, The LHCb trigger and its performance in 2011, J. Instrum. **8**, P04022 (2013).

[58] T. Sjöstrand, S. Mrenna, and P. Skands, A brief introduction to PYTHIA8.1, Comput. Phys. Commun. **178**, 852 (2008); T. Sjöstrand, S. Mrenna, and P. Skands, PYTHIA6.4 physics and manual, J. High Energy Phys. 05 (2006) 026.

[59] I. Belyaev *et al.*, Handling of the generation of primary events in Gauss, the LHCb simulation framework, J. Phys. Conf. Ser. **331**, 032047 (2011).

[60] D. J. Lange, The EVTGEN particle decay simulation package, Nucl. Instrum. Methods Phys. Res., Sect. A **462**, 152 (2001).

[61] N. Davidson, T. Przedzinski, and Z. Was, PHOTOS interface in C++: Technical and physics documentation, Comput. Phys. Commun. **199**, 86 (2016).

[62] A. Ali, P. Ball, L. T. Handoko, and G. Hiller, Comparative study of the decays $B \to (K, K^*)\ell^+\ell^-$ in Standard Model and supersymmetric theories, Phys. Rev. D **61**, 074024 (2000).

[63] S. Descotes-Genon and J. Virto, Time dependence in $B \to V\ell\ell$ decays, J. High Energy Phys. 04 (2015) 045; 07 (2015) 049(E); arXiv:1502.05509.

[64] P. Ball and R. Zwicky, $B_{d,s} \to \rho, \omega, K^*, \phi$ decay form-factors from light-cone sum rules revisited, Phys. Rev. D **71**, 014029 (2005).

[65] J. Allison *et al.* (GEANT4 Collaboration), GEANT4 developments and applications, IEEE Trans. Nucl. Sci. **53**, 270 (2006); S. Agostinelli *et al.* (GEANT4 Collaboration), GEANT4: A simulation toolkit, Nucl. Instrum. Methods Phys. Res., Sect. A **506**, 250 (2003).

[66] M. Clemencic *et al.*, The LHCb simulation application, Gauss: Design, evolution and experience, J. Phys. Conf. Ser. **331**, 032023 (2011).

[67] V. V. Gligorov and M. Williams, Efficient, reliable and fast high-level triggering using a bonsai boosted decision tree, J. Instrum. **8**, P02013 (2013).

[68] T. Likhomanenko *et al.*, LHCb topological trigger reoptimization, J. Phys. Conf. Ser. **664**, 082025 (2015).

[69] S. Navas *et al.* (Particle Data Group), Review of particle physics, Phys. Rev. D **110**, 030001 (2024).

[70] A. V. Dorogush, V. Ershov, and A. Gulin, Catboost: Gradient boosting with categorical features support, arXiv:1810.11363.

[71] A. Blum, A. Kalai, and J. Langford, Beating the hold-out: Bounds for k-fold and progressive cross-validation, in *Proceedings of the Twelfth Annual Conference on Computational Learning Theory, COLT '99* (Association for Computing Machinery, New York, NY, USA, 1999), pp. 203–208, 10.1145/307400.307439.

[72] J. Eschle, A. Puig Navarro, R. Silva Coutinho, and N. Serra, zfit: Scalable pythonic fitting, SoftwareX **11**, 100508 (2020).

[73] N. L. Johnson, Systems of frequency curves generated by methods of translation, Biometrika **36**, 149 (1949).

[74] S. S. Wilks, The large-sample distribution of the likelihood ratio for testing composite hypotheses, Ann. Math. Stat. **9**, 60 (1938).

[75] R. Aaij *et al.* (LHCb Collaboration), Measurements of the branching fraction ratio $\mathcal{B}(\phi \to \mu^+\mu^-)/\mathcal{B}(\phi \to e^+e^-)$ with charm meson decays, J. High Energy Phys. 05 (2024) 293.

[76] B. Efron, Bootstrap methods: Another look at the jackknife, Ann. Stat. **7**, 1 (1979).

[77] D. M. Straub, flavio: A PYTHON package for flavour and precision phenomenology in the standard model and beyond, arXiv:1810.08132.

[78] R. Aaij *et al.* (LHCb Collaboration), Precise measurement of the $f_s/f_d$ ratio of fragmentation fractions and of $B_s^0$ decay branching fractions, Phys. Rev. D **104**, 032005 (2021).

[79] R. Aaij *et al.* (LHCb Collaboration), Constraints on the photon polarisation in $b \to s\gamma$ transitions using $B_s^0 \to \phi e^+e^-$ decays, J. High Energy Phys. 03 (2025) 047.

[80] R. R. Horgan, Z. Liu, S. Meinel, and M. Wingate, Calculation of $B^0 \to K^{*0}\mu^+\mu^-$ and $B_s^0 \to \phi\mu^+\mu^-$ observables using form factors from lattice QCD, Phys. Rev. Lett. **112**, 212003 (2014).

[81] R. R. Horgan, Z. Liu, S. Meinel, and M. Wingate, Rare $B$ decays using lattice QCD form factors, Proc. Sci., LATTICE2014 (**2015**) 372 [arXiv:1501.00367].

[82] R. Aaij *et al.* (LHCb Collaboration), Measurement of the $B_s^0 \to \phi\phi$ branching fraction and search for the decay $B^0 \to \phi\phi$, J. High Energy Phys. 10 (2015) 053.

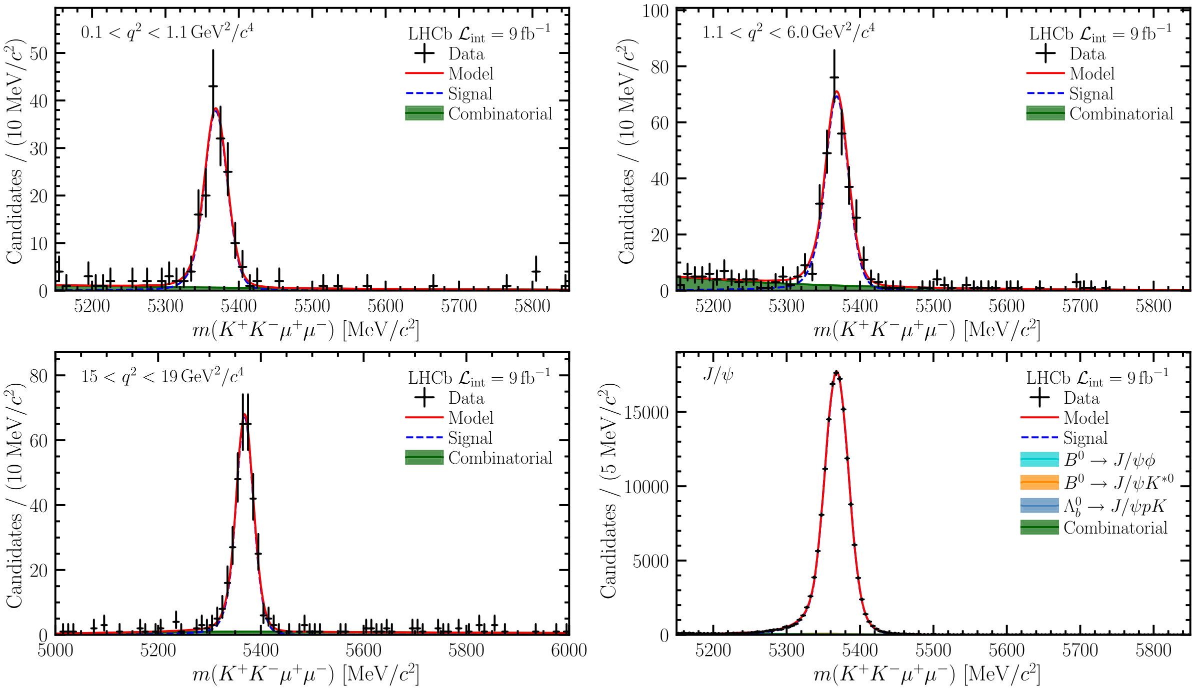

FIG. 3. Mass distributions of selected $B_s^0 \to \phi\mu^+\mu^-$ candidates in the (top left) low-, (top right) central-, (bottom left) high-$q^2$, and (bottom right) $J/\psi$ bins. The data are summed over the three run periods and are compared with the result of the fit described in the text.

## End Matter

*Appendix A: Mass fits for $B_s^0 \to \phi\mu^+\mu^-$ decays*—Figure 3 shows the mass distributions of selected $B_s^0 \to \phi\mu^+\mu^-$ candidates in the different $q^2$ bins. The significant difference in mass resolution between $B_s^0 \to \phi\mu^+\mu^-$ and $B_s^0 \to \phi e^+e^-$ decays, where the latter, shown in Fig. 1, is due to bremsstrahlung from the $e^\pm$ and the imperfect nature of the bremsstrahlung recovery.

*Appendix B: Differential branching fraction of the $B_s^0 \to \phi e^+e^-$ decay*—Figure 4 presents a summary of the measured $B_s^0 \to \phi e^+e^-$ branching fraction from this Letter, compared with that of the $B_s^0 \to \phi\mu^+\mu^-$ decay [4] and predictions based on the SM extracted from Ref. [77] with uncertainties following Refs. [6,80,81].

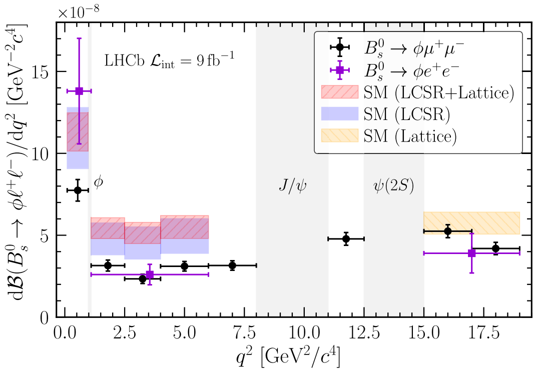

FIG. 4. Differential branching fraction of the $B_s^0 \to \phi e^+e^-$ decay in bins of $q^2$, compared with measurements from $B_s^0 \to \phi\mu^+\mu^-$ decays in Ref. [4] and SM predictions from FLAVIO [77] using form factors calculated with light-cone sum-rule [6] and lattice QCD techniques [80,81].

R. Aaij,[38] A. S. W. Abdelmotteleb,[57] C. Abellan Beteta,[51] F. Abudinén,[57] T. Ackernley,[61] A. A. Adefisoye,[69]
B. Adeva,[47] M. Adinolfi,[55] P. Adlarson,[82] C. Agapopoulou,[14] C. A. Aidala,[83] Z. Ajaltouni,[11] S. Akar,[66]
K. Akiba,[38] P. Albicocco,[28] J. Albrecht,[19,b] F. Alessio,[49] M. Alexander,[60] Z. Aliouche,[63] P. Alvarez Cartelle,[56]
R. Amalric,[16] S. Amato,[3] J. L. Amey,[55] Y. Amhis,[14,49] L. An,[6] L. Anderlini,[27] M. Andersson,[51]
A. Andreianov,[44] P. Andreola,[51] M. Andreotti,[26] D. Andreou,[69] A. Anelli,[31,c] D. Ao,[7] F. Archilli,[37,d]
M. Argenton,[26] S. Arguedas Cuendis,[9,49] A. Artamonov,[44] M. Artuso,[69] E. Aslanides,[13] R. Ataíde Da Silva,[50]
M. Atzeni,[65] B. Audurier,[12] D. Bacher,[64] I. Bachiller Perea,[10] S. Bachmann,[22] M. Bachmayer,[50] J. J. Back,[57]
P. Baladron Rodriguez,[47] V. Balagura,[15] A. Balboni,[26] W. Baldini,[26] L. Balzani,[19] H. Bao,[7]
J. Baptista de Souza Leite,[61] C. Barbero Pretel,[47,12] M. Barbetti,[27] I. R. Barbosa,[70] R. J. Barlow,[63]
M. Barnyakov,[25] S. Barsuk,[14] W. Barter,[59] M. Bartolini,[56] J. Bartz,[69] J. M. Basels,[17] S. Bashir,[40] G. Bassi,[35,e]
B. Batsukh,[5] P. B. Battista,[14] A. Bay,[50] A. Beck,[57] M. Becker,[19] F. Bedeschi,[35] I. B. Bediaga,[2] N. A. Behling,[19]
S. Belin,[47] V. Bellee,[51] K. Belous,[44] I. Belov,[29] I. Belyaev,[36] G. Benane,[13] G. Bencivenni,[28] E. Ben-Haim,[16]
A. Berezhnoy,[44] R. Bernet,[51] S. Bernet Andres,[45] A. Bertolin,[33] C. Betancourt,[51] F. Betti,[59] J. Bex,[56]
Ia. Bezshyiko,[51] J. Bhom,[41] M. S. Bieker,[19] N. V. Biesuz,[26] P. Billoir,[16] A. Biolchini,[38] M. Birch,[62]
F. C. R. Bishop,[10] A. Bitadze,[63] A. Bizzeti, T. Blake,[57] F. Blanc,[50] J. E. Blank,[19] S. Blusk,[69] V. Bocharnikov,[44]
J. A. Boelhauve,[19] O. Boente Garcia,[15] T. Boettcher,[66] A. Bohare,[59] A. Boldyrev,[44] C. S. Bolognani,[79]
R. Bolzonella,[26,f] R. B. Bonacci,[1] N. Bondar,[44] A. Bordelius,[49] F. Borgato,[33,g] S. Borghi,[63] M. Borsato,[31,c]
J. T. Borsuk,[41] S. A. Bouchiba,[50] M. Bovill,[64] T. J. V. Bowcock,[61] A. Boyer,[49] C. Bozzi,[26] A. Brea Rodriguez,[50]
N. Breer,[19] J. Brodzicka,[41] A. Brossa Gonzalo,[47,a] J. Brown,[61] D. Brundu,[32] E. Buchanan,[59] A. Buonaura,[51]
L. Buonincontri,[33,g] A. T. Burke,[63] C. Burr,[49] J. S. Butter,[56] J. Buytaert,[49] W. Byczynski,[49] S. Cadeddu,[32]
H. Cai,[74] A. C. Caillet,[16] R. Calabrese,[26,f] S. Calderon Ramirez,[9] L. Calefice,[46] S. Cali,[28] M. Calvi,[31,c]
M. Calvo Gomez,[45] P. Camargo Magalhaes,[2,h] J. I. Cambon Bouzas,[47] P. Campana,[28] D. H. Campora Perez,[79]
A. F. Campoverde Quezada,[7] S. Capelli,[31] L. Capriotti,[26] R. Caravaca-Mora,[9] A. Carbone,[25,i]
L. Carcedo Salgado,[47] R. Cardinale,[29,j] A. Cardini,[32] P. Carniti,[31,c] L. Carus,[22] A. Casais Vidal,[65] R. Caspary,[22]
G. Casse,[61] M. Cattaneo,[49] G. Cavallero,[26,49] V. Cavallini,[26,f] S. Celani,[22] D. Cervenkov,[64] S. Cesare,[30,k]
A. J. Chadwick,[61] I. Chahrour,[83] M. Charles,[16] Ph. Charpentier,[49] E. Chatzianagnostou,[38] M. Chefdeville,[10]
C. Chen,[13] S. Chen,[5] Z. Chen,[7] A. Chernov,[41] S. Chernyshenko,[53] X. Chiotopoulos,[79] V. Chobanova,[81]
S. Cholak,[50] M. Chrzaszcz,[41] A. Chubykin,[44] V. Chulikov,[28] P. Ciambrone,[28] X. Cid Vidal,[47] G. Ciezarek,[49]
P. Cifra,[49] P. E. L. Clarke,[59] M. Clemencic,[49] H. V. Cliff,[56] J. Closier,[49] C. Cocha Toapaxi,[22] V. Coco,[49]
J. Cogan,[13] E. Cogneras,[11] L. Cojocariu,[43] P. Collins,[49] T. Colombo,[49] M. C. Colonna,[19]
A. Comerma-Montells,[46] L. Congedo,[24] A. Contu,[32] N. Cooke,[60] I. Corredoira,[47] A. Correia,[16] G. Corti,[49]
J. J. Cottee Meldrum,[55] B. Couturier,[49] D. C. Craik,[51] M. Cruz Torres,[2,l] E. Curras Rivera,[50] R. Currie,[59]
C. L. Da Silva,[68] S. Dadabaev,[44] L. Dai,[71] X. Dai,[6] E. Dall'Occo,[49] J. Dalseno,[47] C. D'Ambrosio,[49]
J. Daniel,[11] A. Danilina,[44] P. d'Argent,[24] A. Davidson,[57] J. E. Davies,[63] A. Davis,[63] O. De Aguiar Francisco,[63]
C. De Angelis,[32,m] F. De Benedetti,[49] J. de Boer,[38] K. De Bruyn,[78] S. De Capua,[63] M. De Cian,[22,49]
U. De Freitas Carneiro Da Graca,[2,n] E. De Lucia,[28] J. M. De Miranda,[2] L. De Paula,[3] M. De Serio,[24,o]
P. De Simone,[28] F. De Vellis,[19] J. A. de Vries,[79] F. Debernardis,[24] D. Decamp,[10] V. Dedu,[13] S. Dekkers,[1]
L. Del Buono,[16] B. Delaney,[65] H.-P. Dembinski,[19] J. Deng,[8] V. Denysenko,[51] O. Deschamps,[11] F. Dettori,[32,m]
B. Dey,[77] P. Di Nezza,[28] I. Diachkov,[44] S. Didenko,[44] S. Ding,[69] L. Dittmann,[22] V. Dobishuk,[53]
A. D. Docheva,[60] C. Dong,[4,p] A. M. Donohoe,[23] F. Dordei,[32] A. C. dos Reis,[2] A. D. Dowling,[69] W. Duan,[72]
P. Duda,[80] M. W. Dudek,[41] L. Dufour,[49] V. Duk,[34] P. Durante,[49] M. M. Duras,[80] J. M. Durham,[68]
O. D. Durmus,[77] A. Dziurda,[41] A. Dzyuba,[44] S. Easo,[58] E. Eckstein,[18] U. Egede,[1] A. Egorychev,[44]
V. Egorychev,[44] S. Eisenhardt,[59] E. Ejopu,[63] L. Eklund,[82] M. Elashri,[66] J. Ellbracht,[19] S. Ely,[62] A. Ene,[43]
J. Eschle,[69] S. Esen,[22] T. Evans,[63] F. Fabiano,[32,m] L. N. Falcao,[2] Y. Fan,[7] B. Fang,[7] L. Fantini,[34,49,q]
M. Faria,[50] K. Farmer,[59] D. Fazzini,[31,c] L. Felkowski,[80] M. Feng,[5,7] M. Feo,[19,49] A. Fernandez Casani,[48]
M. Fernandez Gomez,[47] A. D. Fernez,[67] F. Ferrari,[25] F. Ferreira Rodrigues,[3] M. Ferrillo,[51] M. Ferro-Luzzi,[49]
S. Filippov,[44] R. A. Fini,[24] M. Fiorini,[26,f] M. Firlej,[40] K. L. Fischer,[64] D. S. Fitzgerald,[83] C. Fitzpatrick,[63]
T. Fiutowski,[40] F. Fleuret,[15] M. Fontana,[25] L. F. Foreman,[63] R. Forty,[49] D. Foulds-Holt,[56] V. Franco Lima,[3]
M. Franco Sevilla,[67] M. Frank,[49] E. Franzoso,[26,f] G. Frau,[63] C. Frei,[49] D. A. Friday,[63] J. Fu,[7] Q. Führing,[19,56,b]

Y. Fujii,[1] T. Fulghesu,[16] E. Gabriel,[38] G. Galati,[24] M. D. Galati,[38] A. Gallas Torreira,[47] D. Galli,[25,i] S. Gambetta,[59] M. Gandelman,[3] P. Gandini,[30] B. Ganie,[63] H. Gao,[7] R. Gao,[64] T. Q. Gao,[56] Y. Gao,[8] Y. Gao,[6] Y. Gao,[8] L. M. Garcia Martin,[50] P. Garcia Moreno,[46] J. García Pardiñas,[49] K. G. Garg,[8] L. Garrido,[46] C. Gaspar,[49] R. E. Geertsema,[38] L. L. Gerken,[19] E. Gersabeck,[63] M. Gersabeck,[20] T. Gershon,[57] S. G. Ghizzo,[29,j] Z. Ghorbanimoghaddam,[55] L. Giambastiani,[33,g] F. I. Giasemis,[16,r] V. Gibson,[56] H. K. Giemza,[42] A. L. Gilman,[64] M. Giovannetti,[28] A. Gioventù,[46] L. Girardey,[63] P. Gironella Gironell,[46] C. Giugliano,[26,f] M. A. Giza,[41] E. L. Gkougkousis,[62] F. C. Glaser,[14,22] V. V. Gligorov,[16,49] C. Göbel,[70] E. Golobardes,[45] D. Golubkov,[44] A. Golutvin,[62,44,49] S. Gomez Fernandez,[46] W. Gomulka,[40] F. Goncalves Abrantes,[64] M. Goncerz,[41] G. Gong,[4,p] J. A. Gooding,[19] I. V. Gorelov,[44] C. Gotti,[31] J. P. Grabowski,[18] L. A. Granado Cardoso,[49] E. Graugés,[46] E. Graverini,[50,s] L. Grazette,[57] G. Graziani, A. T. Grecu,[43] L. M. Greeven,[38] N. A. Grieser,[66] L. Grillo,[60] S. Gromov,[44] C. Gu,[15] M. Guarise,[26] L. Guerry,[11] M. Guittiere,[14] V. Guliaeva,[44] P. A. Günther,[22] A.-K. Guseinov,[50] E. Gushchin,[44] Y. Guz,[6,44,49] T. Gys,[49] K. Habermann,[18] T. Hadavizadeh,[1] C. Hadjivasiliou,[67] G. Haefeli,[50] C. Haen,[49] J. Haimberger,[49] M. Hajheidari,[49] G. Hallett,[57] M. M. Halvorsen,[49] P. M. Hamilton,[67] J. Hammerich,[61] Q. Han,[8] X. Han,[22,49] S. Hansmann-Menzemer,[22] L. Hao,[7] N. Harnew,[64] M. Hartmann,[14] S. Hashmi,[40] J. He,[7,t] F. Hemmer,[49] C. Henderson,[66] R. D. L. Henderson,[1,57] A. M. Hennequin,[49] K. Hennessy,[61] L. Henry,[50] J. Herd,[62] P. Herrero Gascon,[22] J. Heuel,[17] A. Hicheur,[3] G. Hijano Mendizabal,[51] D. Hill,[50] J. Horswill,[63] R. Hou,[8] Y. Hou,[11] N. Howarth,[61] J. Hu,[72] W. Hu,[6] X. Hu,[4,p] W. Huang,[7] W. Hulsbergen,[38] R. J. Hunter,[57] M. Hushchyn,[44] D. Hutchcroft,[61] M. Idzik,[40] D. Ilin,[44] P. Ilten,[66] A. Inglessi,[44] A. Iniukhin,[44] A. Ishteev,[44] K. Ivshin,[44] R. Jacobsson,[49] H. Jage,[17] S. J. Jaimes Elles,[48,75] S. Jakobsen,[49] E. Jans,[38] B. K. Jashal,[48] A. Jawahery,[67,49] V. Jevtic,[19] E. Jiang,[67] X. Jiang,[5,7] Y. Jiang,[7] Y. J. Jiang,[6] M. John,[64] A. John Rubesh Rajan,[23] D. Johnson,[54] C. R. Jones,[56] T. P. Jones,[57] S. Joshi,[42] B. Jost,[49] J. Juan Castella,[56] N. Jurik,[49] I. Juszczak,[41] D. Kaminaris,[50] S. Kandybei,[52] M. Kane,[59] Y. Kang,[4,p] C. Kar,[11] M. Karacson,[49] D. Karpenkov,[44] A. Kauniskangas,[50] J. W. Kautz,[66] M. K. Kazanecki,[41] F. Keizer,[49] M. Kenzie,[56] T. Ketel,[38] B. Khanji,[69] A. Kharisova,[44] S. Kholodenko,[35,49] G. Khreich,[14] T. Kirn,[17] V. S. Kirsebom,[31,c] O. Kitouni,[65] S. Klaver,[39] N. Kleijne,[35,e] K. Klimaszewski,[42] M. R. Kmiec,[42] S. Koliiev,[53] L. Kolk,[19] A. Konoplyannikov,[44] P. Kopciewicz,[40,49] P. Koppenburg,[38] M. Korolev,[44] I. Kostiuk,[38] O. Kot,[53] S. Kotriakhova, A. Kozachuk,[44] P. Kravchenko,[44] L. Kravchuk,[44] M. Kreps,[57] P. Krokovny,[44] W. Krupa,[69] W. Krzemien,[42] O. Kshyvanskyi,[53] S. Kubis,[80] M. Kucharczyk,[41] V. Kudryavtsev,[44] E. Kulikova,[44] A. Kupsc,[82] B. K. Kutsenko,[13] D. Lacarrere,[49] P. Laguarta Gonzalez,[46] A. Lai,[32] A. Lampis,[32] D. Lancierini,[56] C. Landesa Gomez,[47] J. J. Lane,[1] R. Lane,[55] G. Lanfranchi,[28] C. Langenbruch,[22] J. Langer,[19] O. Lantwin,[44] T. Latham,[57] F. Lazzari,[35,s] C. Lazzeroni,[54] R. Le Gac,[13] H. Lee,[61] R. Lefèvre,[11] A. Leflat,[44] S. Legotin,[44] M. Lehuraux,[57] E. Lemos Cid,[49] O. Leroy,[13] T. Lesiak,[41] E. D. Lesser,[49] B. Leverington,[22] A. Li,[4,p] C. Li,[13] H. Li,[72] K. Li,[8] L. Li,[63] M. Li,[8] P. Li,[7] P.-R. Li,[73] Q. Li,[5,7] S. Li,[8] T. Li,[5,u] T. Li,[72] Y. Li,[8] Y. Li,[5] Z. Lian,[4,p] X. Liang,[69] S. Libralon,[48] C. Lin,[7] T. Lin,[58] R. Lindner,[49] H. Linton,[62] V. Lisovskyi,[50] R. Litvinov,[32,49] F. L. Liu,[1] G. Liu,[72] K. Liu,[73] S. Liu,[5,7] W. Liu,[8] Y. Liu,[59] Y. Liu,[73] Y. L. Liu,[62] A. Lobo Salvia,[46] A. Loi,[32] J. Lomba Castro,[47] T. Long,[56] J. H. Lopes,[3] A. Lopez Huertas,[46] S. López Soliño,[47] Q. Lu,[15] C. Lucarelli,[27] D. Lucchesi,[33,g] M. Lucio Martinez,[79] V. Lukashenko,[38,53] Y. Luo,[6] A. Lupato,[33,v] E. Luppi,[26,f] K. Lynch,[23] X.-R. Lyu,[7] G. M. Ma,[4,p] S. Maccolini,[19] F. Machefert,[14] F. Maciuc,[43] B. Mack,[69] I. Mackay,[64] L. M. Mackey,[69] L. R. Madhan Mohan,[56] M. J. Madurai,[54] A. Maevskiy,[44] D. Magdalinski,[38] D. Maisuzenko,[44] M. W. Majewski,[40] J. J. Malczewski,[41] S. Malde,[64] L. Malentacca,[49] A. Malinin,[44] T. Maltsev,[44] G. Manca,[32,m] G. Mancinelli,[13] C. Mancuso,[30,14,k] R. Manera Escalero,[46] F. M. Manganella,[37] D. Manuzzi,[25] D. Marangotto,[30,k] J. F. Marchand,[10] R. Marchevski,[50] U. Marconi,[25] E. Mariani,[16] S. Mariani,[49] C. Marin Benito,[46,49] J. Marks,[22] A. M. Marshall,[55] L. Martel,[64] G. Martelli,[34,q] G. Martellotti,[36] L. Martinazzoli,[49] M. Martinelli,[31,c] D. Martinez Gomez,[78] D. Martinez Santos,[81] F. Martinez Vidal,[48] A. Martorell i Granollers,[45] A. Massafferri,[2] R. Matev,[49] A. Mathad,[49] V. Matiunin,[44] C. Matteuzzi,[69] K. R. Mattioli,[15] A. Mauri,[62] E. Maurice,[15] J. Mauricio,[46] P. Mayencourt,[50] J. Mazorra de Cos,[48] M. Mazurek,[42] M. McCann,[62] L. Mcconnell,[23] T. H. McGrath,[63] N. T. McHugh,[60] A. McNab,[63] R. McNulty,[23] B. Meadows,[66] G. Meier,[19] D. Melnychuk,[42] F. M. Meng,[4,p] M. Merk,[38,79] A. Merli,[50] L. Meyer Garcia,[67] D. Miao,[5,7] H. Miao,[7] M. Mikhasenko,[76] D. A. Milanes,[75] A. Minotti,[31,c] E. Minucci,[28] T. Miralles,[11] B. Mitreska,[19] D. S. Mitzel,[19] A. Modak,[58]

R. A. Mohammed,[64] R. D. Moise,[17] S. Mokhnenko,[44] E. F. Molina Cardenas,[83] T. Mombächer,[49] M. Monk,[57,1]
S. Monteil,[11] A. Morcillo Gomez,[47] G. Morello,[28] M. J. Morello,[35,e] M. P. Morgenthaler,[22] J. Moron,[40]
W. Morren,[38] A. B. Morris,[49] A. G. Morris,[13] R. Mountain,[69] H. Mu,[4,p] Z. M. Mu,[6] E. Muhammad,[57]
F. Muheim,[59] M. Mulder,[78] K. Müller,[51] F. Muñoz-Rojas,[9] R. Murta,[62] P. Naik,[61] T. Nakada,[50]
R. Nandakumar,[58] T. Nanut,[49] I. Nasteva,[3] M. Needham,[59] N. Neri,[30,k] S. Neubert,[18] N. Neufeld,[49]
P. Neustroev,[44] J. Nicolini,[19,14] D. Nicotra,[79] E. M. Niel,[50] N. Nikitin,[44] P. Nogarolli,[3] P. Nogga,[18]
C. Normand,[55] J. Novoa Fernandez,[47] G. Nowak,[66] C. Nunez,[83] H. N. Nur,[60] A. Oblakowska-Mucha,[40]
V. Obraztsov,[44] T. Oeser,[17] S. Okamura,[26,f] A. Okhotnikov,[44] O. Okhrimenko,[53] R. Oldeman,[32,m] F. Oliva,[59]
M. Olocco,[19] C. J. G. Onderwater,[79] R. H. O'Neil,[59] D. Osthues,[19] J. M. Otalora Goicochea,[3] P. Owen,[51]
A. Oyanguren,[48] O. Ozcelik,[59] F. Paciolla,[35,w] A. Padee,[42] K. O. Padeken,[18] B. Pagare,[57] P. R. Pais,[22]
T. Pajero,[49] A. Palano,[24] M. Palutan,[28] X. Pan,[4,p] G. Panshin,[44] L. Paolucci,[57] A. Papanestis,[58,49]
M. Pappagallo,[24,o] L. L. Pappalardo,[26,f] C. Pappenheimer,[66] C. Parkes,[63] B. Passalacqua,[26,f] G. Passaleva,[27]
D. Passaro,[35,e] A. Pastore,[24] M. Patel,[62] J. Patoc,[64] C. Patrignani,[25,i] A. Paul,[69] C. J. Pawley,[79] A. Pellegrino,[38]
J. Peng,[5,7] M. Pepe Altarelli,[28] S. Perazzini,[25] D. Pereima,[44] H. Pereira Da Costa,[68] A. Pereiro Castro,[47]
P. Perret,[11] A. Perrevoort,[78] A. Perro,[49] K. Petridis,[55] A. Petrolini,[29,j] J. P. Pfaller,[66] H. Pham,[69] L. Pica,[35,e]
M. Piccini,[34] L. Piccolo,[32] B. Pietrzyk,[10] G. Pietrzyk,[14] D. Pinci,[36] F. Pisani,[49] M. Pizzichemi,[31,49,c]
V. Placinta,[43] M. Plo Casasus,[47] T. Poeschl,[49] F. Polci,[16,49] M. Poli Lener,[28] A. Poluektov,[13] N. Polukhina,[44]
I. Polyakov,[44] E. Polycarpo,[3] S. Ponce,[49] D. Popov,[7] S. Poslavskii,[44] K. Prasanth,[59] C. Prouve,[47]
D. Provenzano,[32,m] V. Pugatch,[53] G. Punzi,[35,s] S. Qasim,[51] Q. Q. Qian,[6] W. Qian,[7] N. Qin,[4,p] S. Qu,[4,p]
R. Quagliani,[49] R. I. Rabadan Trejo,[57] J. H. Rademacker,[55] M. Rama,[35] M. Ramírez García,[83]
V. Ramos De Oliveira,[70] M. Ramos Pernas,[57] M. S. Rangel,[3] F. Ratnikov,[44] G. Raven,[39] M. Rebollo De Miguel,[48]
F. Redi,[30,v] J. Reich,[55] F. Reiss,[63] Z. Ren,[7] P. K. Resmi,[64] R. Ribatti,[50] G. R. Ricart,[15,12] D. Riccardi,[35,e]
S. Ricciardi,[58] K. Richardson,[65] M. Richardson-Slipper,[59] K. Rinnert,[61] P. Robbe,[14,49] G. Robertson,[60]
E. Rodrigues,[61] A. Rodriguez Alvarez,[46] E. Rodriguez Fernandez,[47] J. A. Rodriguez Lopez,[75]
E. Rodriguez Rodriguez,[47] J. Roensch,[19] A. Rogachev,[44] A. Rogovskiy,[58] D. L. Rolf,[49] P. Roloff,[49]
V. Romanovskiy,[66] A. Romero Vidal,[47] G. Romolini,[26] F. Ronchetti,[50] T. Rong,[6] M. Rotondo,[28] S. R. Roy,[22]
M. S. Rudolph,[69] M. Ruiz Diaz,[22] R. A. Ruiz Fernandez,[47] J. Ruiz Vidal,[82,x] A. Ryzhikov,[44] J. Ryzka,[40]
J. J. Saavedra-Arias,[9] J. J. Saborido Silva,[47] R. Sadek,[15] N. Sagidova,[44] D. Sahoo,[77] N. Sahoo,[54] B. Saitta,[32,m]
M. Salomoni,[31,49,c] I. Sanderswood,[48] R. Santacesaria,[36] C. Santamarina Rios,[47] M. Santimaria,[28,49] L. Santoro,[2]
E. Santovetti,[37] A. Saputi,[26,49] D. Saranin,[44] A. Sarnatskiy,[78] G. Sarpis,[59] M. Sarpis,[63] C. Satriano,[36,y]
A. Satta,[37] M. Saur,[6] D. Savrina,[44] H. Sazak,[17] F. Sborzacchi,[49,28] L. G. Scantlebury Smead,[64] A. Scarabotto,[19]
S. Schael,[17] S. Scherl,[61] M. Schiller,[60] H. Schindler,[49] M. Schmelling,[21] B. Schmidt,[49] S. Schmitt,[17]
H. Schmitz,[18] O. Schneider,[50] A. Schopper,[49] N. Schulte,[19] S. Schulte,[50] M. H. Schune,[14] R. Schwemmer,[49]
G. Schwering,[17] B. Sciascia,[28] A. Sciuccati,[49] S. Sellam,[47] A. Semennikov,[44] T. Senger,[51] M. Senghi Soares,[39]
A. Sergi,[29,j] N. Serra,[51] L. Sestini,[33] A. Seuthe,[19] Y. Shang,[6] D. M. Shangase,[83] M. Shapkin,[44] R. S. Sharma,[69]
I. Shchemerov,[44] L. Shchutska,[50] T. Shears,[61] L. Shekhtman,[44] Z. Shen,[6] S. Sheng,[5,7] V. Shevchenko,[44]
B. Shi,[7] Q. Shi,[7] Y. Shimizu,[14] E. Shmanin,[25] R. Shorkin,[44] J. D. Shupperd,[69] R. Silva Coutinho,[69] G. Simi,[33,g]
S. Simone,[24,o] N. Skidmore,[57] T. Skwarnicki,[69] M. W. Slater,[54] J. C. Smallwood,[64] E. Smith,[65] K. Smith,[68]
M. Smith,[62] A. Snoch,[38] L. Soares Lavra,[59] M. D. Sokoloff,[66] F. J. P. Soler,[60] A. Solomin,[44,55] A. Solovev,[44]
I. Solovyev,[44] N. S. Sommerfeld,[18] R. Song,[1] Y. Song,[50] Y. Song,[4,p] Y. S. Song,[6] F. L. Souza De Almeida,[69]
B. Souza De Paula,[3] E. Spadaro Norella,[29,j] E. Spedicato,[25] J. G. Speer,[19] E. Spiridenkov,[44] P. Spradlin,[60]
V. Sriskaran,[49] F. Stagni,[49] M. Stahl,[49] S. Stahl,[49] S. Stanislaus,[64] E. N. Stein,[49] O. Steinkamp,[51] O. Stenyakin,[44]
H. Stevens,[19] D. Strekalina,[44] Y. Su,[7] F. Suljik,[64] J. Sun,[32] L. Sun,[74] D. Sundfeld,[2] W. Sutcliffe,[51]
P. N. Swallow,[54] K. Swientek,[40] F. Swystun,[56] A. Szabelski,[42] T. Szumlak,[40] Y. Tan,[4,p] Y. Tang,[74] M. D. Tat,[64]
A. Terentev,[44] F. Terzuoli,[35,49,w] F. Teubert,[49] E. Thomas,[49] D. J. D. Thompson,[54] H. Tilquin,[62] V. Tisserand,[11]
S. T'Jampens,[10] M. Tobin,[5,49] L. Tomassetti,[26,f] G. Tonani,[30,49,k] X. Tong,[6] D. Torres Machado,[2] L. Toscano,[19]
D. Y. Tou,[4,p] C. Trippl,[45] G. Tuci,[22] N. Tuning,[38] L. H. Uecker,[22] A. Ukleja,[40] D. J. Unverzagt,[22] B. Urbach,[59]
E. Ursov,[44] A. Usachov,[39] A. Ustyuzhanin,[44] U. Uwer,[22] V. Vagnoni,[25] V. Valcarce Cadenas,[47] G. Valenti,[25]
N. Valls Canudas,[49] H. Van Hecke,[68] E. van Herwijnen,[62] C. B. Van Hulse,[47,z] R. Van Laak,[50] M. van Veghel,[38]

G. Vasquez,[51] R. Vazquez Gomez,[46] P. Vazquez Regueiro,[47] C. Vázquez Sierra,[47] S. Vecchi,[26] J. J. Velthuis,[55]
M. Veltri,[27,aa] A. Venkateswaran,[50] M. Verdoglia,[32] M. Vesterinen,[57] D. Vico Benet,[64] P. Vidrier Villalba,[46]
M. Vieites Diaz,[49] X. Vilasis-Cardona,[45] E. Vilella Figueras,[61] A. Villa,[25] P. Vincent,[16] F. C. Volle,[54]
D. vom Bruch,[13] N. Voropaev,[44] K. Vos,[79] G. Vouters,[10] C. Vrahas,[59] J. Wagner,[19] J. Walsh,[35] E. J. Walton,[1,57]
G. Wan,[6] C. Wang,[22] G. Wang,[8] J. Wang,[6] J. Wang,[5] J. Wang,[4,p] J. Wang,[74] M. Wang,[30] N. W. Wang,[7]
R. Wang,[55] X. Wang,[8] X. Wang,[72] X. W. Wang,[62] Y. Wang,[6] Z. Wang,[14] Z. Wang,[4,p] Z. Wang,[30] J. A. Ward,[57,1]
M. Waterlaat,[49] N. K. Watson,[54] D. Websdale,[62] Y. Wei,[6] J. Wendel,[81] B. D. C. Westhenry,[55] C. White,[56]
M. Whitehead,[60] E. Whiter,[54] A. R. Wiederhold,[63] D. Wiedner,[19] G. Wilkinson,[64] M. K. Wilkinson,[66]
M. Williams,[65] M. J. Williams,[49] M. R. J. Williams,[59] R. Williams,[56] Z. Williams,[55] F. F. Wilson,[58] M. Winn,[12]
W. Wislicki,[42] M. Witek,[41] L. Witola,[22] G. Wormser,[14] S. A. Wotton,[56] H. Wu,[69] J. Wu,[8] X. Wu,[74] Y. Wu,[6]
Z. Wu,[7] K. Wyllie,[49] S. Xian,[72] Z. Xiang,[5] Y. Xie,[8] A. Xu,[35] J. Xu,[7] L. Xu,[4,p] L. Xu,[4,p] M. Xu,[57] Z. Xu,[49]
Z. Xu,[7] Z. Xu,[5] D. Yang,[4] K. Yang,[62] S. Yang,[7] X. Yang,[6] Y. Yang,[29,j] Z. Yang,[6] Z. Yang,[67]
V. Yeroshenko,[14] H. Yeung,[63] H. Yin,[8] X. Yin,[7] C. Y. Yu,[6] J. Yu,[71] X. Yuan,[5] Y Yuan,[5,7] E. Zaffaroni,[50]
M. Zavertyaev,[21] M. Zdybal,[41] F. Zenesini,[25,i] C. Zeng,[5,7] M. Zeng,[4,p] C. Zhang,[6] D. Zhang,[8] J. Zhang,[7]
L. Zhang,[4,p] S. Zhang,[71] S. Zhang,[64] Y. Zhang,[6] Y. Z. Zhang,[4,p] Y. Zhao,[22] A. Zharkova,[44] A. Zhelezov,[22]
S. Z. Zheng,[6] X. Z. Zheng,[4,p] Y. Zheng,[7] T. Zhou,[6] X. Zhou,[8] Y. Zhou,[7] V. Zhovkovska,[57] L. Z. Zhu,[7]
X. Zhu,[4,p] X. Zhu,[8] V. Zhukov,[17] J. Zhuo,[48] Q. Zou,[5,7] D. Zuliani,[33,g] and G. Zunica[50]

(LHCb Collaboration)

[1]*School of Physics and Astronomy, Monash University, Melbourne, Australia*
[2]*Centro Brasileiro de Pesquisas Físicas (CBPF), Rio de Janeiro, Brazil*
[3]*Universidade Federal do Rio de Janeiro (UFRJ), Rio de Janeiro, Brazil*
[4]*Department of Engineering Physics, Tsinghua University, Beijing, China, Beijing, China*
[5]*Institute Of High Energy Physics (IHEP), Beijing, China*
[6]*School of Physics State Key Laboratory of Nuclear Physics and Technology, Peking University, Beijing, China*
[7]*University of Chinese Academy of Sciences, Beijing, China*
[8]*Institute of Particle Physics, Central China Normal University, Wuhan, Hubei, China*
[9]*Consejo Nacional de Rectores (CONARE), San Jose, Costa Rica*
[10]*Université Savoie Mont Blanc, CNRS, IN2P3-LAPP, Annecy, France*
[11]*Université Clermont Auvergne, CNRS/IN2P3, LPC, Clermont-Ferrand, France*
[12]*Université Paris-Saclay, Centre d¿Etudes de Saclay (CEA), IRFU, Saclay, France, Gif-Sur-Yvette, France*
[13]*Aix Marseille Univ, CNRS/IN2P3, CPPM, Marseille, France*
[14]*Université Paris-Saclay, CNRS/IN2P3, IJCLab, Orsay, France*
[15]*Laboratoire Leprince-Ringuet, CNRS/IN2P3, Ecole Polytechnique, Institut Polytechnique de Paris, Palaiseau, France*
[16]*LPNHE, Sorbonne Université, Paris Diderot Sorbonne Paris Cité, CNRS/IN2P3, Paris, France*
[17]*I. Physikalisches Institut, RWTH Aachen University, Aachen, Germany*
[18]*Universität Bonn - Helmholtz-Institut für Strahlen und Kernphysik, Bonn, Germany*
[19]*Fakultät Physik, Technische Universität Dortmund, Dortmund, Germany*
[20]*Physikalisches Institut, Albert-Ludwigs-Universität Freiburg, Freiburg, Germany*
[21]*Max-Planck-Institut für Kernphysik (MPIK), Heidelberg, Germany*
[22]*Physikalisches Institut, Ruprecht-Karls-Universität Heidelberg, Heidelberg, Germany*
[23]*School of Physics, University College Dublin, Dublin, Ireland*
[24]*INFN Sezione di Bari, Bari, Italy*
[25]*INFN Sezione di Bologna, Bologna, Italy*
[26]*INFN Sezione di Ferrara, Ferrara, Italy*
[27]*INFN Sezione di Firenze, Firenze, Italy*
[28]*INFN Laboratori Nazionali di Frascati, Frascati, Italy*
[29]*INFN Sezione di Genova, Genova, Italy*
[30]*INFN Sezione di Milano, Milano, Italy*
[31]*INFN Sezione di Milano-Bicocca, Milano, Italy*
[32]*INFN Sezione di Cagliari, Monserrato, Italy*
[33]*INFN Sezione di Padova, Padova, Italy*
[34]*INFN Sezione di Perugia, Perugia, Italy*
[35]*INFN Sezione di Pisa, Pisa, Italy*

[36]INFN Sezione di Roma La Sapienza, Roma, Italy
[37]INFN Sezione di Roma Tor Vergata, Roma, Italy
[38]Nikhef National Institute for Subatomic Physics, Amsterdam, Netherlands
[39]Nikhef National Institute for Subatomic Physics and VU University Amsterdam, Amsterdam, Netherlands
[40]AGH - University of Krakow, Faculty of Physics and Applied Computer Science, Kraków, Poland
[41]Henryk Niewodniczanski Institute of Nuclear Physics Polish Academy of Sciences, Kraków, Poland
[42]National Center for Nuclear Research (NCBJ), Warsaw, Poland
[43]Horia Hulubei National Institute of Physics and Nuclear Engineering, Bucharest-Magurele, Romania
[44]Affiliated with an institute covered by a cooperation agreement with CERN
[45]DS4DS, La Salle, Universitat Ramon Llull, Barcelona, Spain
[46]ICCUB, Universitat de Barcelona, Barcelona, Spain
[47]Instituto Galego de Física de Altas Enerxías (IGFAE), Universidade de Santiago de Compostela, Santiago de Compostela, Spain
[48]Instituto de Fisica Corpuscular, Centro Mixto Universidad de Valencia—CSIC, Valencia, Spain
[49]European Organization for Nuclear Research (CERN), Geneva, Switzerland
[50]Institute of Physics, Ecole Polytechnique Fédérale de Lausanne (EPFL), Lausanne, Switzerland
[51]Physik-Institut, Universität Zürich, Zürich, Switzerland
[52]NSC Kharkiv Institute of Physics and Technology (NSC KIPT), Kharkiv, Ukraine
[53]Institute for Nuclear Research of the National Academy of Sciences (KINR), Kyiv, Ukraine
[54]School of Physics and Astronomy, University of Birmingham, Birmingham, United Kingdom
[55]H.H. Wills Physics Laboratory, University of Bristol, Bristol, United Kingdom
[56]Cavendish Laboratory, University of Cambridge, Cambridge, United Kingdom
[57]Department of Physics, University of Warwick, Coventry, United Kingdom
[58]STFC Rutherford Appleton Laboratory, Didcot, United Kingdom
[59]School of Physics and Astronomy, University of Edinburgh, Edinburgh, United Kingdom
[60]School of Physics and Astronomy, University of Glasgow, Glasgow, United Kingdom
[61]Oliver Lodge Laboratory, University of Liverpool, Liverpool, United Kingdom
[62]Imperial College London, London, United Kingdom
[63]Department of Physics and Astronomy, University of Manchester, Manchester, United Kingdom
[64]Department of Physics, University of Oxford, Oxford, United Kingdom
[65]Massachusetts Institute of Technology, Cambridge, Massachusetts, USA
[66]University of Cincinnati, Cincinnati, Ohio, USA
[67]University of Maryland, College Park, Maryland, USA
[68]Los Alamos National Laboratory (LANL), Los Alamos, New Mexico, USA
[69]Syracuse University, Syracuse, New York, USA
[70]Pontifícia Universidade Católica do Rio de Janeiro (PUC-Rio), Rio de Janeiro, Brazil
(associated with Universidade Federal do Rio de Janeiro (UFRJ), Rio de Janeiro, Brazil)
[71]School of Physics and Electronics, Hunan University, Changsha City, China
(associated with Institute of Particle Physics, Central China Normal University, Wuhan, Hubei, China)
[72]Guangdong Provincial Key Laboratory of Nuclear Science, Guangdong-Hong Kong Joint Laboratory of Quantum Matter,
Institute of Quantum Matter, South China Normal University, Guangzhou, China
(associated with Department of Engineering Physics, Tsinghua University, Beijing, China, Beijing, China)
[73]Lanzhou University, Lanzhou, China
(associated with Institute Of High Energy Physics (IHEP), Beijing, China)
[74]School of Physics and Technology, Wuhan University, Wuhan, China
(associated with Department of Engineering Physics, Tsinghua University, Beijing, China, Beijing, China)
[75]Departamento de Fisica, Universidad Nacional de Colombia, Bogota, Colombia
(associated with LPNHE, Sorbonne Université, Paris Diderot Sorbonne Paris Cité, CNRS/IN2P3, Paris, France)
[76]Ruhr Universitaet Bochum, Fakultaet f. Physik und Astronomie, Bochum, Germany
(associated with Fakultät Physik, Technische Universität Dortmund, Dortmund, Germany)
[77]Eotvos Lorand University, Budapest, Hungary
(associated with European Organization for Nuclear Research (CERN), Geneva, Switzerland)
[78]Van Swinderen Institute, University of Groningen, Groningen, Netherlands
(associated with Nikhef National Institute for Subatomic Physics, Amsterdam, Netherlands)
[79]Universiteit Maastricht, Maastricht, Netherlands
(associated with Nikhef National Institute for Subatomic Physics, Amsterdam, Netherlands)
[80]Tadeusz Kosciuszko Cracow University of Technology, Cracow, Poland
(associated with Henryk Niewodniczanski Institute of Nuclear Physics Polish Academy of Sciences, Kraków, Poland)
[81]Universidade da Coruña, A Coruña, Spain
(associated with DS4DS, La Salle, Universitat Ramon Llull, Barcelona, Spain)

[82]*Department of Physics and Astronomy, Uppsala University, Uppsala, Sweden*
*(associated with School of Physics and Astronomy, University of Glasgow, Glasgow, United Kingdom)*
[83]*University of Michigan, Ann Arbor, Michigan, USA*
*(associated with Syracuse University, Syracuse, New York, USA)*

[a] Deceased.

[b] Also at Lamarr Institute for Machine Learning and Artificial Intelligence, Dortmund, Germany.

[c] Also at Università degli Studi di Milano-Bicocca, Milano, Italy.

[d] Also at Università di Roma Tor Vergata, Roma, Italy.

[e] Also at Scuola Normale Superiore, Pisa, Italy.

[f] Also at Università di Ferrara, Ferrara, Italy.

[g] Also at Università di Padova, Padova, Italy.

[h] Also at Facultad de Ciencias Fisicas, Madrid, Spain.

[i] Also at Università di Bologna, Bologna, Italy.

[j] Also at Università di Genova, Genova, Italy.

[k] Also at Università degli Studi di Milano, Milano, Italy.

[l] Also at Universidad Nacional Autónoma de Honduras, Tegucigalpa, Honduras.

[m] Also at Università di Cagliari, Cagliari, Italy.

[n] Also at Centro Federal de Educacão Tecnológica Celso Suckow da Fonseca, Rio De Janeiro, Brazil.

[o] Also at Università di Bari, Bari, Italy.

[p] Also at Center for High Energy Physics, Tsinghua University, Beijing, China.

[q] Also at Università di Perugia, Perugia, Italy.

[r] Also at LIP6, Sorbonne Université, Paris, France.

[s] Also at Università di Pisa, Pisa, Italy.

[t] Also at Hangzhou Institute for Advanced Study, UCAS, Hangzhou, China.

[u] Also at School of Physics and Electronics, Henan University, Kaifeng, China.

[v] Also at Università di Bergamo, Bergamo, Italy.

[w] Also at Università di Siena, Siena, Italy.

[x] Also at Department of Physics/Division of Particle Physics, Lund, Sweden.

[y] Also at Università della Basilicata, Potenza, Italy.

[z] Also at Universidad de Alcalá, Alcalá de Henares, Spain.

[aa] Also at Università di Urbino, Urbino, Italy.